Relativistic effects in physics and chemistry of element 105. I. Periodicities in properties of group 5 elements. Electronic structure of the pentachlorides

V. Pershina,[a] W.-D. Sepp, and B. Fricke
Theoretical Physics Department, University of Kassel, 3500 Kassel, Germany

A. Rosén
Chalmers University of Technology and University of Göteborg, S-41296 Göteborg, Sweden

(Received 25 November 1991; accepted 13 February 1992)

A detailed study of the electronic structure and bonding of the pentahalides of group 5 elements V, Nb, Ta, and element 105, hahnium (and Pa) has been carried out using relativistic molecular cluster Dirac–Slater discrete-variational method. A number of calculations have been performed for different geometries and molecular bond distances. The character of the bonding has been analyzed using the Mulliken population analysis of the molecular orbitals. It is shown that hahnium is a typical group 5 element. In a great number of properties it continues trends in the group. Some peculiarities in the electronic structure of $HaCl_5$ result from relativistic effects.

I. INTRODUCTION

It is known that near the end of the periodic table relativistic effects play an important role in determining atomic characteristics such as binding energies, atomic (ionic) radii, etc. This finally influences the physics and chemistry of the heavy and superheavy elements leading to peculiarities in their chemical behavior.

Early relativistic calculations for atoms and ions[1,2] have already shown that there is a strong relativistic stabilization of $s_{1/2}$ and $p_{1/2}$ orbitals as function of atomic number and, as a secondary effect, destabilization of d orbitals and their spatial expansion. Multiconfiguration Dirac–Fock (MCDF) calculations[3,4,5] have shown that change of the spatial extension of orbitals in a relativistic treatment compared to a nonrelativistic one leads to different ground state electronic configurations for Lr and element 104 than those which would be expected on the basis of a straightforward extrapolation of the periodic system. Lr turned out to have a $7s^27p_{1/2}$ ground state electronic configuration instead of the expected $7s^26d$ one and 104 to have $7s^27p_{1/2}6d$ instead of $7s^26d^2$. First excited configurations of Lr($7s^26d$) and of element 104 ($6d^27d^2$) are by 0.19 and 0.24 eV, respectively, higher.

A number of chemical experiments[6,7] were carefully planned to provide some evidence for the groud state electronic configurations of these elements and to observe the periodicities in their properties as a consequence of relativistic effects. Thus, e.g., the experiments[6] on the volatility of element 103 as a possible analog of p-element Tl failed to confirm this idea and it was not possible to reduce the trivalent Lr to the monovalent state.[7] This reduction was expected owing to strong "inert pair" effect of the $7s^2$ electrons.

The other two groups of experiments which studied volatility of the elements 103, 104, and 105 and their halides using the gas chromatography technique[8,9,10] and the solution chemistry experiments which investigated the process of complex formation by the exchange solvent extraction[11,12,13] have given strong evidence that the actinide series ends at Lr and that a new series begins with element 104. Element 104 was found to be an analog of the group 4 elements and 105 an analog of the group 5 elements and their chemical behavior was characteristic of the elements of these groups.

These experiments however revealed that the properties within the groups are not changing smoothly and that there is a break in periodicity and, as it was supposed in Ref. 13, even a reversal, as in the case of solvent extraction of the element 105 complexes. In the experiments on the gas phase chemistry of elements 104 and 105 halides, it has been found that the 104 chloride and bromide are more volatile than their analogs MCl_4 and MBr_4 (M = Zr, Hf)[9(b)-9(d),10(a)] while the 105 chloride and bromide are substantially less volatile compared to MCl_5 and MBr_5 (M = Nb, Ta).[10(a),10(e),10(f)] These interesting experimental results need to be given some theoretical interpretation and the general analogy between the transition elements within the groups is worth being considered independently.

Chemical properties of the transition elements of the first, second, and third row in general resemble each other while the members of the last two rows are different from the elements of the first row by a number of characteristics. These are atomic, ionic, and metallic radii; oxidation states (oxidation potentials); stereochemistry of ions in solutions or solid state; crystal-field, spin–orbital effects and magnetic properties. Thus to talk about analogy within the groups one should consider first these characteristics taking into account the fact that with increasing relativistic effects down columns of the periodic table some simple extrapolations of chemical properties may no longer be a reliable approach.[14]

[a] Permanent address: 117915 Moscow, Leninski pr. 31, Institute of Physical Chemistry, Russian Academy of Sciences.

 0021-9606/92/118367-12$06.00

Subtle, individual effects, configuration mixing can play an important role leading to changes in the periodicities.

In order to discuss the chemistry of element 105 we start with a summary of what is known from relativistic atomic calculations for V, Nb, Ta, and Ha. (This review is presented in Sec. II). The chemical bonding in group 5 elements compounds (and Pa for comparison) has been studied by us for the pentachlorides MCl_5, with M = V, Nb, Ta, Ha, and Pa. A number of relativistic molecular cluster calculations have been performed for different geometries and moleculer bond distances. Section III gives a brief introduction in the Dirac–Slater discrete-variational method with self-consistent charge approximation (SCC-DS-DVM) and computational details of the molecular calculations. The results of the calculations are presented in Sec. IV where the character of the bonding is analyzed by the Mulliken population analysis of the molecular orbitals. The possibility of Ha forming a pentachloride in C_{4v} geometrical configuration is discussed in Sec. V. General conclusions about trends in group 5 are presented in Sec. VI.

II. RELATIVISTIC ATOMIC CALCULATIONS AS A BASIS FOR PREDICTING THE CHEMICAL PROPERTIES

From relativistic self-consistent field (SCF) atomic calculations some predictions can be made about chemical properties of the heavy elements and their analogs. Results of the atomic calculations together with available experimental data for the group 5 elements are given in Table I. From this table one can see that a dominating ground state electronic configuration in group 5 is d^3s^2 with the exception of Nb. For element 105 the MCDF calculations[5(c)] prove the ground state electronic configuration to be $6d^37s^2$ (with 87.1% configuration weight). So the MCDF calculations have confirmed the ground state electronic configuration of Ha which was predicted in the earlier calculations.[1,2] Thus element 105 is expected to be a d element with properties being determined mainly by valence $7s$ and $6d$ orbitals.

Both Dirac–Slater[1] and recent MCDF calculations[5(c)] have shown that there is an increase in atomic and ionic radii from Ta to 105. For the pentavalent state of V, Nb, Ta, and 105 the R_{max} data as a result of calculations[5(c)] are given in Table I. These values have been normalized and extrapolated to the experimental ionic radii. Ionization potentials (0) − (5 +) decrease in going from V to Ha (see Table I). Thus because of the probably larger ionic and covalent radii and the small ionization energy element 105 will readily reach its maximum oxidation state. In this oxidation state it should therefore be a quite hard Lewis acid with low polarizability. It should be only a little bit softer than the $5d$-elements in the same oxidation state.

Atomic electronic structure data (atomic, ionic radii, ionization potentials, maxima of radial charge densities) change smoothly from Nb to Ta and to element 105. So the chemical properties of element 105 should resemble the properties of its analogs Nb and Ta with peculiarities determined by the type of compound involved.

The strength of chemical bonding is determined by energies of the atomic shells and their spatial distribution. The spatial distribution of the valence ns and $(n-1)d$ orbitals change within the group in different ways. Because of the relativistic contraction of the ns orbitals the maximum in the radial charge density function decreases from Nb to 105. Thus for the neutral V, Nb, Ta, and 105 these values are 1.54, 1.68, 1.53, and 1.45 Å. The $(n-1)d$ functions on the contrary become more expanded in going from Nb to 105 (e.g., 0.456, 0.745, 0.804, and 0.908 Å for the three positively charged V, Nb, Ta, and Ha). The two diametrically opposed behavior of the valence ns and $np_{1/2}$ orbitals on the one hand and $(n-1)d$ and $np_{3/2}$ orbitals on the other hand could result in local effects giving rise to strengthening or weakening the chemical bond in a particular case depending whether the energy of the $(n-1)d$ orbital is above or below those of the other valence orbitals.

Energy eigenvalues of the valence ns and $(n-1)d$

TABLE I. Some physicochemical data for group 5 elements V, Nb, Ta, Ha, and for Pa.

Property	V	Nb	Ta	Ha	Pa	Reference
Ground state configuration	$3d^34s^2$	$4d^45s$	$5d^36s^2$	$6d^37s^{2a}$	$5f^26d7s^2$	15(a)
First excited configuration	$3d^44s$	$4d^35s^2$	$5d^46s$	···	$5f6d^27s^2$	15(a)
Excitation energy (eV)	0.26	0.14	1.21	···	0.25[b]	15(a)
$R_{max}(M^{5+})$ (Å)	0.435	0.586	0.604	0.685	0.865	5(c)
Ionic radius (M^{5+}) (Å) (CN = 6)	0.54	0.64	0.64	0.74[a]	0.78	17
Experimental ionization potential (0 − 5 +) (eV)	162.64	135.05	132.03[c]	126.38[c]	···	15(b)
Calculated ionization potential (0 − 5 +) (eV)	158.43	129.55	126.14	121.00	110.14[d]	5(c)

[a] Reference 5(c).
[b] Reference 16.
[c] Normalized and extrapolated [Ref. 5(c)] to the experimental values.
[d] Reference 18.

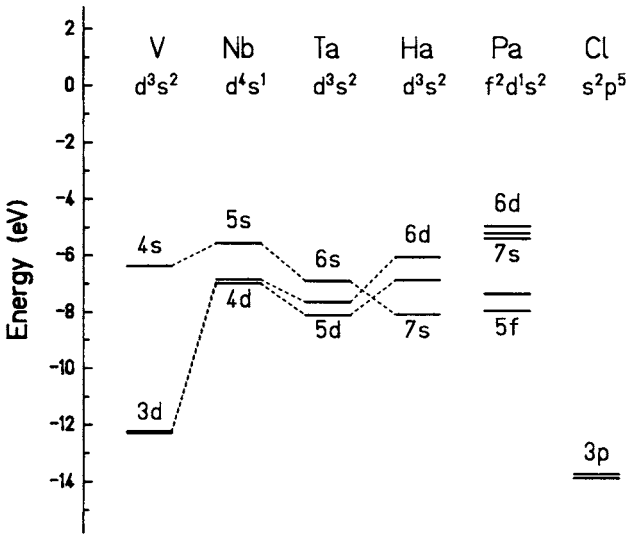

FIG. 1. Binding energies of ns and $(n-1)d$ AOs for V, Nb, Ta, Ha, Pa, and Cl (Ref. 19).

atomic orbitals (AOs) as a result of DF calculations[19] are shown in Fig. 1. From this figure one can see that there is relativistic stabilization of ns AOs and destabilization of $(n-1)d$ ones as a secondary effect in going from V to Ha. Spin–orbital splitting of $(n-1)d$ AOs increases as well in this direction. Hahnium having $7s$ and $6d$ AOs in nearly the same energy region as ns and $(n-1)d$ orbitals of Nb and Ta will have different contributions to bonding of these orbitals compared to those of Nb and Ta. Protactinium has less stabilized $7s$ and $6d$ orbitals compared to hahnium with $5f$ AOs being also in the valence region and taking part in chemical bonding. Taking into consideration the important information from the relativistic atomic calculations molecular relativistic quantum-chemical calculations can nevertheless provide a basis for better understanding the nature of chemical bonding in particular cases.

III. METHOD AND COMPUTATIONAL DETAILS OF THE MOLECULAR CALCULATIONS

A. SCC-DS-DV method

Dirac–Slater calculations of the molecular electronic structure of the group 5 halides have been performed using the relativistic DVM with SCC approximation as developed by Rosen and Ellis.[20]

The four-component basis functions Φ_j are symmetry orbitals which are determined through a linear-combination-of-atomic-orbitals (LCAO) expansion, i.e.,

$$\Phi_j = \sum_q W_q \begin{Bmatrix} [P_{nk}(r)/r]\, Y_{km}(\mathbf{r},\xi) \\ [iQ_{nk}(r)/r]\, Y_{-km}(\mathbf{r},\xi) \end{Bmatrix}, \tag{1}$$

where $P_{nk}(r)$ and $Q_{nk}(r)$ are the big and small components of numerical relativistic atomic (DS) wave functions; $Y_{km}(\mathbf{r},\xi)$ are vector-coupled spin harmonics; W_q represents the expansion of the symmetry orbitals.

The quantum number k is defined as

$$k = -(l+1) \text{ when } j = (l+1/2)$$

and

$$k = l \text{ for } j = (l-1/2).$$

The molecular integrals between the basis functions are calculated in a numerical three-dimensional grid. The Hamiltonian matrix elements are given by

$$h_{i,j} = \sum_k w_k \Phi_i^*(\mathbf{r}_k) h_D \Phi_j(\mathbf{r}_k), \tag{2}$$

where w_k is the weight factor for grid point $\mathbf{r}_k$ and h_D is the Dirac Hamiltonian

$$h_D = c\alpha\mathbf{p} + (\beta - 1)c^2 + V. \tag{3}$$

The potential V is the sum of three parts,

$$V = V_n + V_C + V_x,$$

with V_n being the nuclear, V_C the Coulomb, and $V_x = -3\alpha(3\rho/8\pi)^{1/3}$ the exchange potentials. The diagonalization of

$$(\mathbf{h} - \epsilon_i \mathbf{S})\mathbf{c}_i = 0 \tag{4}$$

gives the molecular orbitals (MOs)

$$\Psi_i = \sum_j c_j \Phi_j.$$

The symmetry molecular orbitals for double point groups were constructed using the projection operator method[21] implemented into the program.[22] The program includes time reversal invariance resulting in additional selection rules in the nonrelativistic limit. The calculations have been done both within the all-electron and the frozen core approximations in which symmetry orbitals are constructed for the core and valence regions. The symmetry orbitals for the valence region are then orthogonalized to the core orbitals in the first iteration and kept frozen in the following iterations.

The basis set has been varied to investigate its influence on the electronic structure data. Minimal as well as ionized basis sets were used to test the change of the eigenvalues. The extended basis set including valence $np_{1/2}$ and $np_{3/2}$ orbitals was used to examine the influence of these orbitals on the chemical bond formation. The results on the charge density distribution presented in the paper are for the neutral basis set. The trends in these values within the group are the same for the ionized basis. Numerical integration was done using 9000 integration points.

During the SCC procedure charge density functionals are generated via orbital occupations found by the Mulliken charge analysis of the occupied molecular orbitals.

Mulliken population analysis has been used to analyze the charge density distribution data.[23] In a single determinant N-electron wave function built up from orthogonal molecular orbitals, the charge density in terms of symmetry orbitals is given as

$$\rho(\mathbf{r}) = \sum_{j,k} \Phi_i^*(\mathbf{r}) \Phi_k(\mathbf{r}) t_{jk},$$

where

$$t_{jk} = \sum_i c_{ji}^* c_{ki}.$$

Following Mulliken[23] the total number of electrons N is

$$N = \int \rho(\mathbf{r}) d\tau = \sum_{j,k} S_{jk} t_{jk},$$

where $S_{jk} = \int \Phi_j^* \Phi_k d\tau$ is the symmetry orbital overlap matrix.

To analyze the chemical bonding it is important to break up the molecular electron density according to Mulliken into the following constituents. The net atomic population of an orbital j on center r contributing to molecular orbital i is defined as

$$n(i;j_r) = N(i) c_{ij_r}^2,$$

where c_{ij} are MO coefficients for atomic orbital j on center r and $N(i)$ is the occupation of the ith MO. Then summation over all MOs gives

$$n(j_r) = \sum_i n(i;j_r),$$

and summation over all orbitals in atom r gives

$$n(r) = \sum_i n(j_r).$$

Here c_{ij_r} are MO coefficients obtained in the solution of the secular Eq. (4).

Gross atomic population of orbital j_r, contributing to molecular orbital i, is expressed as

$$N(i;j_r) = N(i) c_{ij_r} \left(c_{ij_r} + \sum_{s \neq r} c_{ik_s} S_{j_r k_s} \right).$$

Summation over all MOs gives gross atomic orbital populations

$$N(j_r) = \sum_i N(i;j_r)$$

and finally the effective charge of any AO (or in other words AO population)

$$q(j_r) = N_0(j_r) - N(j_r),$$

where $N_0(j_r)$ is the number of electrons in the AO Φ_j.

The different partial overlap populations are

$$n(i;j_r,k_s) = 2N(i) c_{ij_r} c_{ik_r} S_{j_r k_s},$$

$$n(j_r,k_s) = \sum_i n(i;j_r,k_s),$$

$$n(i) = \sum_{j_r k_s} n(i;j_r,k_s),$$

between orbitals j and k on the centers r and s. The total overlap population is

$$n = \sum_i n(i) = \sum_{r,s} n(r,s) = \sum_{j_r k_s} n(j_r,k_s).$$

These different overlap populations have been widely used to analyze the chemical bonding taking into account the fact that the overlap population is a counterpart of the covalent bond energy.[23] We recite here the Mulliken expression of the MO energy via the overlap population parameter

TABLE II. Input geometrical parameters, bond distances $R_{M\text{-}Cl}$ and Cl_{ax}–M–Cl angle (C_{4v}) for MCl_5.

	V[b]	Nb[a]	Ta[a]	Ha[b]	Pa[b]
Symmetry	D_{3h}	D_{3h}	D_{3h}	D_{3h}	C_{4v}
$R_{M\text{-}Cl_{ax}}$ (Å)	2.21	2.338	2.369	2.45; 2.42[c]	2.44 (104°)
$R_{M\text{-}Cl_{eq}}$ (Å)	2.18	2.241	2.227	2.31; 2.28[c]	2.44 (104°)

[a] Reference 24.
[b] Estimated values.
[c] Bond lengths with relativistic contraction.

$$N(i)\epsilon_i = \sum_{j_r} N(i;j_r)\alpha(j_r) + \sum_{s>r} n(i;j_r,k_s)[\beta(j_r,k_s)/S(j_r,k_s)].$$

Here $\beta(j_r,k_s)$ is the overlap energy and $\alpha(j_r)$ the Coulomb energy parameters.

B. Input parameters for MCl_5 (M=V, Nb, Ta, Ha, and Pa)

It is known that Nb and Ta form rather volatile pentachlorides existing in the gas phase as monomers. Electron diffraction study[24] have shown that they have geometrical configuration of a trigonal bipyramid possessing D_{3h} symmetry according to Fig. 2(a) with the interatomic distances listed in Table II.

Protactinium pentahalides have also been calculated because Pa is often included in the experiments as a possible analog whose properties sometimes resemble the properties of the group 5 elements. Unfortunately no data are available in the literature about structures of the protactinium pentahalides in the gas phase. It is however known that Pa in most cases forms solid state compounds typical of the early actinides and especially uranium. The solid state structure of $PaCl_5$ for example is similar to that of UCl_5. Such a similarity in structures between UCl_5 and $PaCl_5$ should be expected also in the gas phase. In an earlier work (Ref. 25) we analyzed electronic structure of the gas phase UF_5 as a square pyramid of C_{4v} symmetry with uranium atom above the planar square. This geometry and not a D_{3h} one has been predicted for gaseous UF_5 in Ref. 26 by the analysis of the infrared spectrum. By analogy we have investigated the structures for $PaCl_5$ of C_{4v} symmetry [see Fig. 2(b)], with

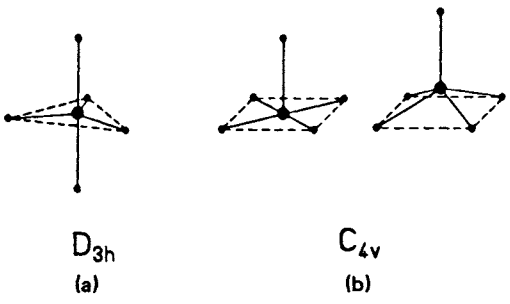

FIG. 2. Geometrical structure of MCl_5 molecules.

the D_{3h} symmetry being also included in the calculations for comparison. For element 105 we considered two possible structures, D_{3h} symmetry according to the d^3sp hybridization and C_{4v} symmetry according to the d^2sp^2 one. The bond lengths for $PaCl_5$ were estimated on the basis of the solid-state structural data.[27] The internuclear distances for the 105 halides were varied in a range from 2.30 to 2.55 Å.

Results for 105 chlorides are mainly presented for R_{ax}/R_{eq} equal to 2.45/2.31 and 2.42/2.28 Å. The first distances were estimated taking into account the differences in the ionic radii between element 105 and analogs obtained from MCDF calculations[5(c)] and the second ones from an assumption of the relativistic contraction of the bond length owing to a strong contribution of the 7*s*-orbitals to the chemical bonding (see Sec. IV). (In the latter case the increases in the bond lengths in $HaCl_5$ compared to $TaCl_5$ were taken as an average between those values for $104H_4$ and $106H_6$ compared to HfH_4 and WH_6 obtained in Ref. 28.)

IV. RESULTS AND DISCUSSION

A. Protactinium pentahalides

Despite the fact that Pa in many of its compounds exists in a pentavalent state and easily forms the double bond with oxygen in compounds as $PaOL_x$ it can hardly be considered as an analog of the group 5 elements. Protactinium is a member of the *f*-element series with the $5f^26d^17s^2$ ground state electronic configuration. Its properties are determined by the *f*, *d*, and *s* electrons and by hybridization of these orbitals. As was mentioned before, the D_{3h} hybridization is not typical for the *f*-elements and UF_5 does not exist in the gas phase in this form.

Our calculations of the electronic structure of $PaCl_5$ in D_{3h} symmetry with bond distances equal to 2.44 Å have shown that this geometry is not the proper one. The total overlap population for $PaCl_5$ in this geometry is negative which means that the molecule in this shape is not stable due to the repulsion between the atoms. While interaction of the central atom with two axial ligands gives bonding with overlap population between them equal to 0.23 the three equatorial ligands interact in a repulsive way with the metal atom giving negative overlap population of -1.31. So the resulting total overlap between central atom and ligands is negative (-1.08). This unreal distribution of the electron density within the molecule gives meaningless values of the effective charges and atomic occupancies. The results on $PaCl_5$ in C_{4v} symmetry on the contrary show quite reasonable values which will be discussed later with total overlap population being equal to 1.96.

B. Pentachlorides of the group 5*d*-elements

The detailed analysis of the electronic structure of $HaCl_5$ and comparison with the analogs $NbCl_5$, $TaCl_5$ have mainly been done in D_{3h} symmetry. For comparison the hypothetic molecule VCl_5 has also been included in the calculations. The possible C_{4v} symmetry for $HaCl_5$ will be discussed in Sec. V.

1. Overview of the molecular eigenvalues

In Fig. 3 the general splitting of the orbitals in the ligand fields of D_{3h} and C_{4v} symmetries is shown (without a scale) in relativistic and nonrelativistic representations.

The energy level diagram for the pentachlorides of V, Nb, Ta, Ha, and Pa is shown in Fig. 4(a). The relative ordering of the molecular levels depends on relative level positions for the constituent atoms, the crystal-field splitting, and covalency effect. The results show that all the *d*-elements pentachlorides have similar energy level structure. The set of binding levels ends with levels of predominantly 3*p*-character of Cl and separated from them by the energy gap are vacant *d* levels of the metal. The energy gap ΔE increases in going from VCl_5 to $HaCl_5$ [see Fig. 4(b)] owing to the relative destabilization of the *d* orbitals. The crystal-field splitting of *d* orbitals increases as well along the series.

2. Analysis of the bonding character of the molecular levels

The molecular orbital eigenvalues of Nb, Ta, Ha, and Pa are given in Table III. MO bond orders and compositions are given elsewhere.[29] The occupied orbitals of the $NbCl_5$, $TaCl_5$, and $HaCl_5$ can be divided into several groups. The six highest ones are essentially nonbonding halogen *p*-type orbitals. Below them are three orbitals responsible for rather weak interaction between valence *np* metal orbitals and 3*p* chlorine ones. From MO composition[29] it is interesting to see that from Nb to Ta and to Ha the $np_{1/2}$ orbital contribution decreases while the $np_{3/2}$ one increases. The orbital (20D7) contributing to the (*ns*)metal–ligand bonding in $NbCl_5$ is above the five $(n-1)d$-ligand (18D7–15D9) bonding orbitals while in $TaCl_5$ and $HaCl_5$ this orbital

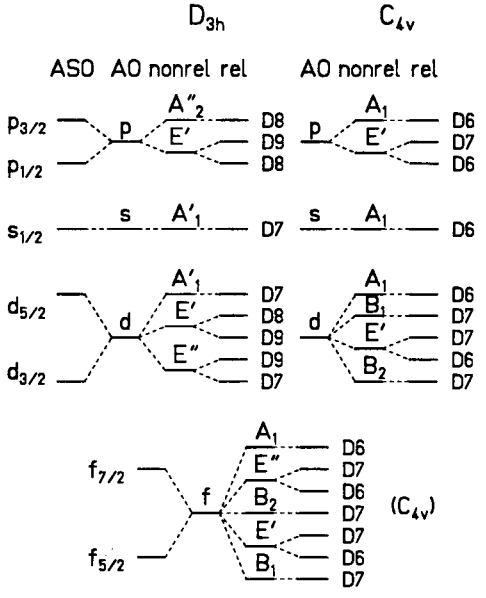

FIG. 3. General splitting of *s*, *p*, *d*, and *f* orbitals in ligand fields of D_{3h} and C_{4v} symmetries.

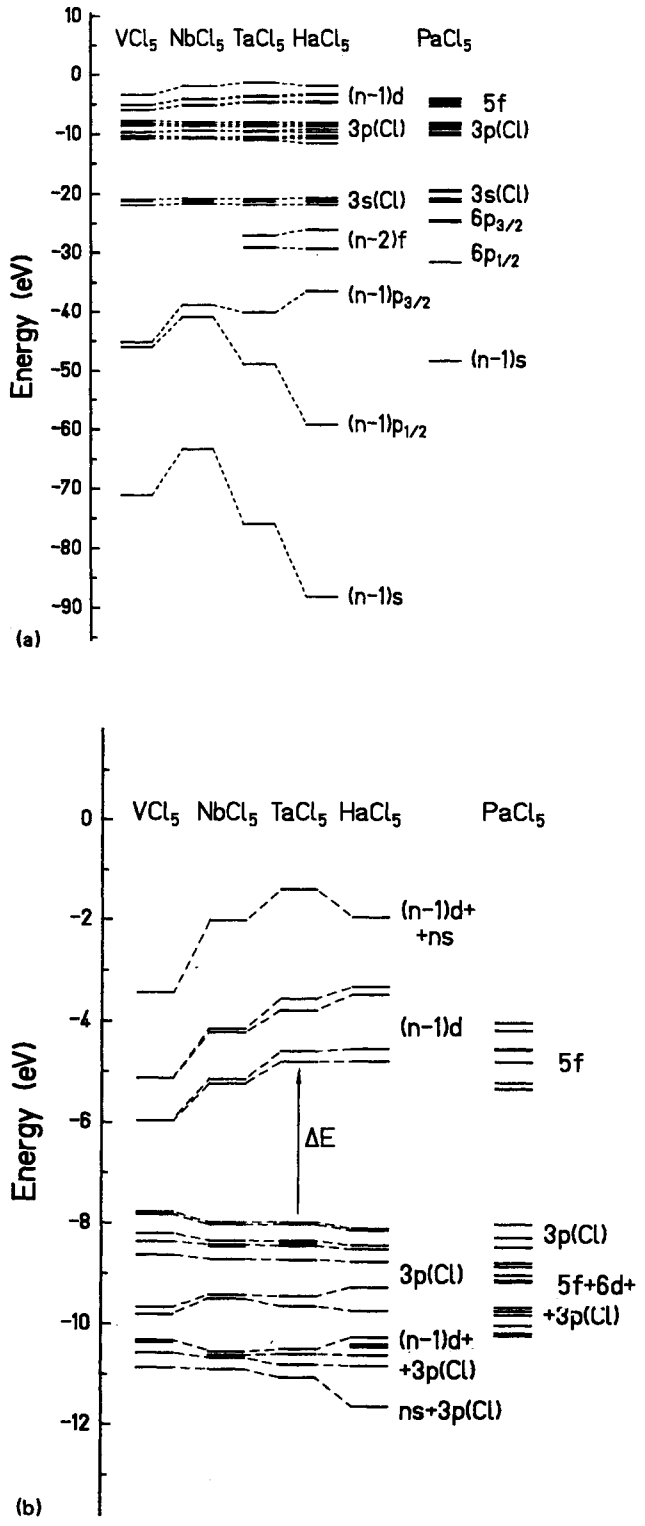

FIG. 4. (a) Energy level structure for MCl_5 molecules. (b) Highest occupied and lowest vacant energy levels.

(24D7 and 30D7, respectively) is below the five bonding MOs (19D9–26D7 for $TaCl_5$ and 24D9–25D9 for $HaCl_5$) between $(n-1)d$ metal orbitals and the chlorine ones. These five MOs are mainly responsible for the bonding between metal atom and ligands (see Ref. 29). The diffusity

TABLE III. Molecular orbital eigenvalues for MCl_5.

$NbCl_5$		$TaCl_5$		$HaCl_5$[a]		$PaCl_5$	
Orbital	Energy (eV)	Orbital	Energy (eV)	Orbital	Energy (eV)	Orbital	Energy (eV)
...	...	...	...	...	...	53D6	4.03
...	...	...	...	...	...	42D7	4.18
24D7	1.99	30D7	1.18	36D7	1.44	52D6	4.55
24D8	3.97	29D8	3.31	34D8	3.12	41D7	4.56
20D9	4.04	25D9	3.53	30D9	3.30	40D7	4.79
19D9	5.14	24D9	4.55	29D9	4.45	51D6	5.21
23D7	5.23	29D7	4.78	35D7	4.77	39D7	5.33
18D9	7.93	23D9	7.90	28D9	8.02	50D6	8.02
22D7	7.97	28D7	7.93	34D7	8.07	38D7	8.29
17D9	8.27	22D9	8.16	27D9	8.21	49D6	8.49
23D8	8.28	28D8	8.20	33D8	8.26	48D6	8.78
22D8	8.36	27D8	8.31	32D8	8.40	37D7	8.79
21D7	8.91	27D7	9.02	33D7	9.03	36D7	8.85
21D8	9.48	26D8	9.57	31D8	9.39	47D6	9.03
16D9	9.51	21D9	9.60	26D9	9.42	35D7	9.13
20D8	9.55	25D8	9.79	30D8	9.91	46D6	9.16
20D7	10.53	26D7	10.52	25D9	10.35	34D7	9.67
15D9	10.62	20D9	10.57	32D7	10.38	45D6	9.74
19D7	10.66	25D7	10.67	31D7	10.70	44D6	9.82
14D9	10.78	24D8	10.87	29D8	10.76	43D6	10.03
19D8	10.80	19D9	10.92	24D9	10.93	33D7	10.20
18D7	10.84	24D7	11.22	30D7	11.74	32D7	10.25
18D8	20.59	23D8	20.47	28D8	20.43	31D7	19.32
17D7	20.99	23D7	20.86	29D7	20.89	42D6	19.60

[a] For $R = 2.45/2.32$ Å.

and destabilization of $6d$ orbitals of Ha are the reason of their more complicated involvement into bonding with the final result being shown in the tables of partial and total overlap populations. Below these levels are MOs of predominantly $3s$(Cl) character with slight admixture of nd(metal) orbitals. The lower lying levels are nearly pure metal orbitals not participating in bonding.

An interesting behavior however show the vacant orbitals of d character [see Fig. 4(b)]. Besides the fact that the general scheme of d orbital splitting in the crystal field of D_{3h} symmetry is preserved for all the molecules under consideration the increase in the d orbital splitting from $NbCl_5$ to $TaCl_5$ is broken by the drastic decrease in energy of 36D7 MO in case of $HaCl_5$. The reason is that in fact 36D7 MO is no more an orbital of d character. The drastic increase in the $7s$ AO content of this highest MO from 3.8% to 4.4% and to 57.6% in going from $NbCl_5$ to $TaCl_5$ and to $HaCl_5$ (see Ref. 29) owing to the relativistic stabilization of the $7s$ AO results in the stabilization of this MO. This will finally influence some physicochemical properties, e.g., energies of highest electron charge-transfer transitions. Supposing that the same effect is presented for hahnium compounds with partially filled $6d$ shell the energies of the highest electronic d–d transitions will be lower in $HaCl_5$ compared to $TaCl_5$.

Total and partial density of states (PDOS) diagrams [see Figs. 5(a) and 5(b)] can be also used to establish the redistribution of atomic character over the binding energy spectra. The PDOS corresponding to a particular atomic

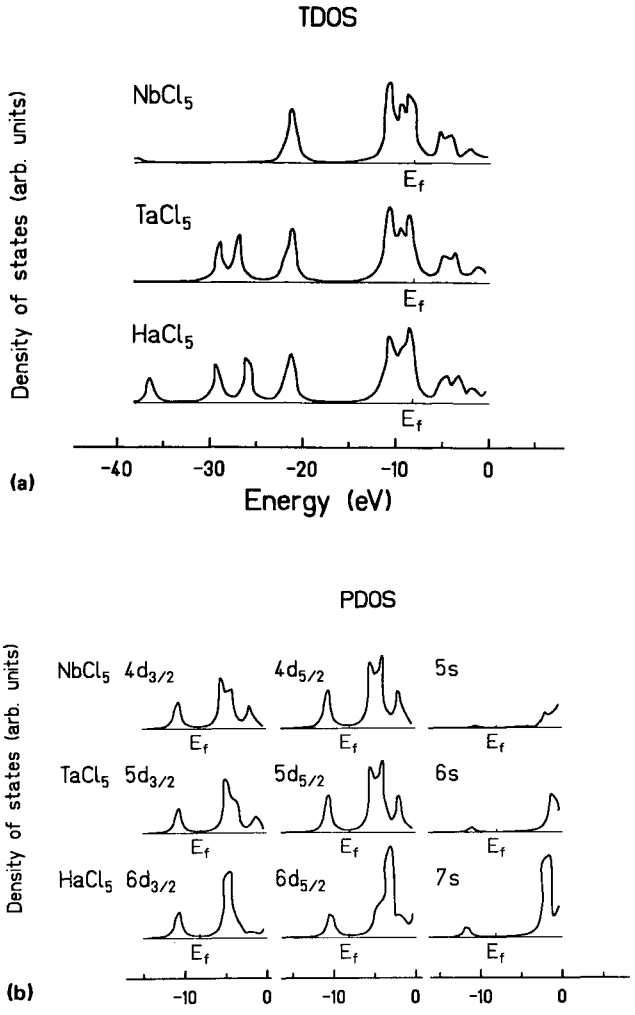

FIG. 5. (a) Total and (b) partial densities of states in MCl_5 (M = Nb, Ta, and Ha).

orbital can be obtained by weighting MO energy levels by the Mulliken orbital population q_j for each state. Then the discrete level structure of the cluster is broadened by introducing a Lorentzian linewidth to obtain a pictorial representation.

Thus Fig. 5(a) shows bonding components of the valent orbitals resulting from covalent mixing of metal orbitals with $3p$(Cl) AOs as well as lines of $3s$(Cl) and $(n-2)f$ AOs for $TaCl_5$ and $HaCl_5$. The $(n-1)d_{3/2}$ and $(n-1)d_{5/2}$ PDOS [see Fig. 5(b)] show the crystal-field splittings with those for $HaCl_5$ being not pronounced due to the strong $7s$ contribution to the highest vacant MOs which was discussed before. In addition one can see that the contribution of the $d_{5/2}$ AOs into bonding decreases in going from $NbCl_5$ to $HaCl_5$ while that of ns AOs increases (ns PDOS). The ns PDOS shows also increasing contribution of ns orbitals to the vacant orbital region drastically changing the character of the highest antibonding MOs.

The nature of chemical bonding is different in $PaCl_5$ [see Table III, Ref. 29, and Fig. 4]. The set of bonding MOs is separated from vacant orbitals of $5f$ character by the energy gap ΔE which is more narrow than that of the d-element pentahalides. The crystal field splitting of the $5f$ orbitals is less than that of the d-elements due to lower spatial distribution of $5f$ orbitals compared to the d ones.

The last occupied MO is purely nonbonding 100% (Cl). The chemical bonding is mainly done by nearly equal participation of $5f$ and $6d$ orbitals of protactinium. It is also substantially influenced by the $6p$ orbital participation. Because of the strong spin–orbital splitting of the $6p$ orbital into $6p_{1/2}$ and $6p_{3/2}$ components the latter acts in an antibonding way destabilizing rather high 38D7 and 49D6 MOs. (The $6p_{3/2}$ orbital contributes to a great extent to 31D7 and 42D6 MOs giving the negative overlap metal–ligand.)

3. Analysis of the atomic populations

The effective atomic charges and occupancies of the valence s, p, d, and f orbitals as a result of calculations are shown in Table IV. Here we show first nl contributions. From this table one can see that the changes in the bond distances do not give any significant change in the charge density distribution data (as in the case of $HaCl_5$). Thus some conclusions about chemical bonding can be done without knowing the equilibrium bond distance.

The effective atomic charges within the group do not change smoothly from one element to another. There is a general decrease in values of effective atomic charges with a break on Ta. The atomic orbital populations change rather smoothly from $NbCl_5$ to $HaCl_5$; q_s and q_p increase while q_d decreases. The q_j values for the relativistic atomic orbitals (Table V) show that the behavior of the orbitals is basically in agreement with the contraction of s and $p_{1/2}$ functions and an expansion of $p_{3/2}$ and d functions for heavier elements as was shown by the earlier discussion of atomic (ionic) radii, etc. Nevertheless the changes in the stabilization or destabilization of some of nlj orbitals are not a smooth function of atomic number. Thus gradual relativistic stabilization of $np_{1/2}$ valence orbitals in going from Nb pentachloride to Ha

TABLE IV. Effective charges on atoms (Q) and atomic orbital populations (q_l) for MCl_5.

Molecule	$R_{M\text{-}Cl_{ax}}$ (Å) / $R_{M\text{-}Cl_{eq}}$ (Å)	Q	q_s	q_p	q_d	q_f	ΔE (eV)
VCl_5[a]	2.21 / 2.18	1.12	0.24	0.36	3.27	···	1.81
$NbCl_5$	2.338 / 2.241	0.93	0.20	0.22	3.65	···	2.70
$TaCl_5$	2.369 / 2.227	0.95	0.35	0.33	3.37	13.99	3.10
$HaCl_5$	2.42 / 2.28	0.81	0.55	0.33	3.32	13.99	3.36
$HaCl_5$	2.45 / 2.31	0.80	0.58	0.34	3.29	13.99	3.25
$HaCl_5$	2.47 / 2.32	0.79	0.60	0.35	3.27	13.99	3.18
$PaCl_5$	2.44	0.98	0.13	0.13	2.09	1.70	2.68

[a] For comparison molecule VCl_5 is also included in Table IV.

TABLE V. Relativistic atomic orbital populations (q_j) for MCl_5.

Orbital	$NbCl_5$	$TaCl_5$	$HaCl_5$ 2.45/2.31 Å	$HaCl_5$ 2.42/2.28 Å	$PaCl_5$[a]
$s_{1/2}$	0.20	0.35	0.58	0.55	0.13
$p_{1/2}$	0.08	0.15	0.22	0.22	0.07
$p_{3/2}$	0.14	0.18	0.12	0.11	0.06
$d_{3/2}$	1.51	1.45	1.53	1.54	0.91
$d_{5/2}$	2.14	1.92	1.76	1.78	1.18

[a] For $PaCl_5$, $q(5f_{5/2}) = 0.83$ and $q(5f_{7/2}) = 0.86$.

gives rise to an increase in $q(p_{1/2})$ while destabilization of $p_{3/2}$ orbitals is not gradual with increasing atomic number and Ta has relatively stabilized $6p_{3/2}$ AO. The $(n-1)d_{3/2}$ orbital which is supposed to be gradually destabilized along the series has the biggest occupation in $HaCl_5$. Orbitals $(n-1)d_{5/2}$ are gradually destabilized along the series.

4. Analysis of the orbital overlap

The different behavior of the metal valence orbitals brings some peculiarities into their bonding with valence orbitals of ligands. The data on partial overlap populations of these orbitals with all chlorine orbitals are presented in Table VI.

From Table VI one can see that the valence orbitals contribute to the chemical bonding in a different way and the contribution of some of them is not a smooth function of atomic number. Thus relativistic stabilization of $ns_{1/2}$ orbitals with increasing atomic number results in a bond strengthening owing to increase in $(ns_{1/2})$metal–ligand overlap which is especially pronounced in the case of Ha. Valence $np_{1/2}$ orbitals have the same effect and it is worth noticing that the contribution of $7p_{1/2}$ orbitals of Ha in the total overlap is ~9.4% and is twice that of $5p_{1/2}$ orbitals in the case of Nb.

The behavior of $np_{3/2}$ orbitals is the most interesting one. From $NbCl_5$ to $TaCl_5$ this orbital contributes more to bonding. In case of $HaCl_5$ it is highly destabilized and contributes to the bonding even to a lesser extent than the $5p_{3/2}$ orbital of Nb. This process leads finally to the total overlap population of $7p_{1/2}$ and $7p_{3/2}$ AOs being intermediate between those of Nb and Ta.

Destabilization of $d_{3/2}$ and $d_{5/2}$ orbitals as a secondary relativistic effect should have resulted in diminishing the overlap population between these orbitals and the orbitals of ligands, but in reality the strong space expansion of these orbitals (as it was shown with R_{max}) results in the increase in their contribution to bonding. Nevertheless the relative contribution of d orbitals to bonding decreases from Nb to Ha as can be seen from Table VII. Thus all these complicated processes give rise to redistribution of the electron density in going from $NbCl_5$ to $HaCl_5$ so that $s_{1/2}$ and $p_{1/2}$ orbitals contribute relatively more to bonding while the contribution of d orbitals decreases (Table VII).

In the case of $PaCl_5$ one can see that the valence orbitals overlap in a different way compared to the d-element pentachlorides and $HaCl_5$ in particular. Having the same principal quantum number as Ha the valence orbitals of protactinium contribute differently to bonding. The $7s$(Pa) orbital is not so strongly overlapping with ligands as the $7s$ orbital of hahnium, which is also the case for $7p$ orbitals. The $6d$ orbitals overlap rather well with the chlorines as well as $5f$ ones. Nevertheless the total metal–ligand overlap is much lower than that in the d-element chlorides because of the strong negative overlap of the $6p$ orbitals of Pa with orbitals of chlorines $[n(6p_{1/2} - \mathrm{Cl}) = -0.25$ and $n(6p_{3/2} - \mathrm{Cl}) = -0.89]$.

This different behavior of different valence AOs as a function of atomic number explains the nongradual diminishing of the values of the effective charges from Nb to Ta and further to Ha. In going from Nb to Ta the increase in electron density on the metal atom gained by relativistic stabilization of s and $p_{1/2}$ orbitals is compensated by the decrease in density on $p_{3/2}$ and d orbitals owing to their destabilization. As a result the value of Q in Ta and Nb is nearly equal. Then in Ha halide $6d$ orbitals are only a little bit more destabilized than in Ta in contrast with their high destabilization in Ta compared to Nb. This little destabilization is highly covered by strong stabilization of $7s$ AO in Ha and its

TABLE VI. Partial overlap populations of the valence metal orbitals with all chlorine orbitals for MCl_5.

Orbital	$NbCl_5$	$TaCl_5$	$HaCl_5$ 2.45/2.31 Å	$HaCl_5$ 2.42/2.28 Å	$PaCl_5$[a]
$s_{1/2}$	0.28	0.41	0.48	0.48	0.19
$p_{1/2}$	0.14	0.22	0.30	0.29	0.12
$p_{3/2}$	0.24	0.30	0.21	0.20	0.11
p(tot)	0.38	0.52	0.50	0.49	0.23
$d_{3/2}$	0.83	0.84	0.85	0.87	0.83
$d_{5/2}$	1.25	1.28	1.30	1.33	1.19
d(tot)	2.08	2.12	2.16	2.19	2.01
The sum	2.74	3.05	3.14	3.16	2.30

[a] In case of $PaCl_5$ $n(f_{5/2} - \mathrm{Cl}) = 0.44$ and $n(f_{7/2} - \mathrm{Cl}) = 0.57$; $6p$-orbitals give negative overlap population of 1.15 so that the total value for overlap metal–ligand is 2.30.

TABLE VII. Relative contributions of the valence metal orbitals (in %) in covalent bonding for MCl_5.

Orbital	$NbCl_5$	$TaCl_5$	$HaCl_5$ 2.45/2.31 Å	$HaCl_5$ 2.42/2.28 Å	$PaCl_5$[a]
$s_{1/2}$	10.1	13.5	15.4	15.1	5.5
$p_{1/2}$	5.0	7.3	9.4	9.2	3.5
$p_{3/2}$	8.9	9.9	6.6	6.3	3.3
p(tot)	13.9	17.2	16.0	15.6	6.7
$d_{3/2}$	30.3	27.5	27.2	27.4	23.9
$d_{5/2}$	45.8	41.9	41.5	41.9	34.4
d(tot)	76.1	69.4	68.7	69.4	58.3

[a] In case of $PaCl_5$ the relative contributions of $f_{5/2}$ and $f_{7/2}$ orbitals in the total overlap are 13.0% and 16.5%, respectively.

TABLE VIII. Contributions to the binding energy for MCl_5.[a]

MCl_5	Q	p_i	E_i (eV)	n_c	E_c (eV)	ion (%)	ΔH_{diss} (eV)
Nb	0.93	0.19	5.22	2.04	12.58	29.32	17.80[c]
Ta	0.95	0.20	5.54	2.49	13.71	28.78	19.25[c]
Pa	0.98	0.22	5.71	1.97	12.30	29.33	19.47[c]
Ha[b]	0.81	0.14	3.83	2.60	13.94	21.55	17.76[d]

[a] Q is the effective charge on an atom; p_i is the ionic bond order equal to $\Sigma - Q(k)Q(l)(a_0/R)$; E_i is the ionic contribution to binding (dissociation) energy equal to $-ne^2Q_MQ_L/R_{M\text{-}L}$ (eV); n_c is the covalent bond order; E_c is the covalent (overlap) energy; ion is ionicity in %.
[b] Data for $R = 2.45/2.31$ Å.
[c] Calculated from Born–Haber cycle.
[d] Estimated from present MO calculations.

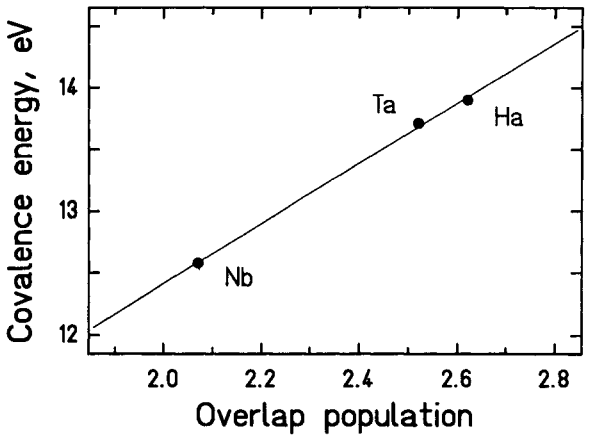

FIG. 7. Correlation between overlap population n and covalence part of the binding energy for MCl_5.

high population so that the final increase of electron density on the Ha atom is the reason of its lower effective charge.

5. Estimation of the chemical bond strength

The total Mulliken population analysis data (effective charges, ionic, and covalent bond orders) are presented in Table VIII.

From these data one can see how the character of the chemical bond is changing along the series. The compounds are predominantly covalent what is in line with earlier conclusions based on experimental data.[30] Nevertheless covalency changes not smoothly from Nb to Ta and further to Ha. There is pronounced increase from Nb to Ta while $HaCl_5$ is only a little bit more covalent than $TaCl_5$. The ionicity on the contrary is nearly equal for $NbCl_5$ and $TaCl_5$ while $HaCl_5$ is obviously less ionic. $PaCl_5$ has much lower covalent contribution to binding compared to the d-element pentachlorides.

Data of Table VIII can be used to evaluate the chemical bond strength for $HaCl_5$. Here effective charges Q, ionic bond orders p_i, ionic contributions to binding energy E_i, and covalent bond orders n_c have been obtained from the present MO calculations. Dissociation energies ΔH_{diss} for $NbCl_5$, $TaCl_5$, and $PaCl_5$ were estimated from the Born–Haber cycle (Fig. 6) using experimental data[30,31] for ΔH_{subl} of metals, molecules MCl_5, ΔH_{form} for solid MCl_5 and ΔH_{diss} for Cl_2. (The data for $PaCl_5$ are not consistent.)[27,32] The atomization energy $D = -\Delta H_{diss}$ is the sum of covalent (overlap) energy, ionic bonding energy, and energy of ionic–covalent resonance. Using ΔH_{diss} for $NbCl_5$ and $TaCl_5$ and the ionic part of the dissociation energy (E_i), the covalent part was estimated (E_c). Then taking into account the fact that overlap population is a direct counterpart of the covalent energy the correlation between these two values was used (Fig. 7) to estimate E_c for $HaCl_5$. Together with the ionic part it gives the enthalpy of dissociation for $HaCl_5$ equal to 17.76 eV.

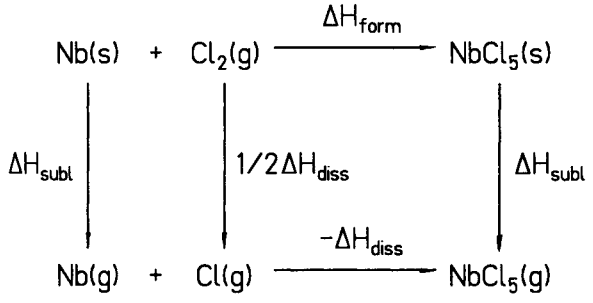

FIG. 6. Born–Haber cycle for MCl_5 formation.

6. Ionization potentials, electron affinities, and energies of electron transitions

Some other characteristics of electronic structure such as ionization potentials, electron affinity, and electron charge-transfer transitions have also been calculated using transition state procedure.[33] The results are shown in Table IX.

Transition-state calculations show that the energy gap increases in going from $NbCl_5$ to $HaCl_5$. This finally will result in an increase in the energies of electronic charge-transfer transitions from occupied MO of Cl-type to the vacant orbitals of metal character. (With increasing interatomic distances in $HaCl_5$ this value decreases.) Electron affinity decreases from $NbCl_5$ to $HaCl_5$ (in case of the short bond length for $HaCl_5$). Obviously stability of MCl_5 towards the process of reduction increases in direction to Ha chloride provided short bond lengths are realized in the hahnium pentachloride. Correlation between oxidation potentials $E^0(V - IV)$[34] and the energies of lowest charge-transfer transitions for V, Nb, Ta, and Ha (see Fig. 8) gives the value $E^0(V - IV)$ for hahnium between -1.00 and -1.15 V, depending on the interatomic distances in $HaCl_5$.

TABLE IX. Ionization potentials (IP), electron affinities (EA), and energies of electron charge-transfer transitions ($E_{\pi\text{-}d}$) for MCl_5 (eV).

Parameter	$NbCl_5$	$TaCl_5$	$HaCl_5$ 2.42/2.28 Å	$HaCl_5$ 2.45/2.31 Å	$HaCl_5$ 2.47/2.32 Å
HOMO[a]	18D9	23D9	28D9	28D9	28D9
Energy	7.93	7.90	8.04	8.02	8.02
IP	10.77	10.73	10.83	10.75	10.71
LUMO[a]	23D7	29D7	35D7	35D7	35D7
Energy	5.23	4.78	4.60	4.77	4.84
EA	2.04	1.53	1.49	1.62	1.71
Transition	18D9→23D7	23D9→29D7	28D9→35D7	28D9→35D7	28D9→35D7
$E_{\pi\text{-}d}$ as an energy difference	2.70	3.10	3.36	3.25	3.18
$E_{\pi\text{-}d}$ via transition state	2.98	3.41	3.70	3.50	3.43

[a] HOMO is the highest occupied molecular orbital; LUMO is the lowest unoccupied molecular orbital.

V. OTHER POSSIBLE GEOMETRICAL STRUCTURES FOR $HaCl_5$

Notwithstanding the fact that analogs of $HaCl_5$—$NbCl_5$ and $TaCl_5$—exist in the gas phase in the form of a trigonal pyramid (D_{3h}) alternative geometrical configurations of $HaCl_5$ as a square pyramide with the central atom in the planar square and above it [see Fig. 2(b)] have also been considered. The C_{4v} symmetry could possibly be realized due to d^2sp^2 hybridization of the valence orbitals. The results of our calculations show that for the same average bond distances (of 2.37 Å) the charge density distribution in $HaCl_5$ (C_{4v}) is nearly the same as in $HaCl_5$ (D_{3h}) with Q effective equal to 0.81 and q_{6d}, q_{7s}, and q_{7p} equal to 3.27, 0.59, and 0.34, respectively. This can be compared with the values of Q and q_l for $HaCl_5$ in D_{3h} symmetry (Table IV). In both cases the electron density distribution is close to pure d^3sp hybridization. The energy gap between occupied and vacant levels of metal character which in a way is a measure of stability of a compound is somewhat bigger in the case of $HaCl_5$ (D_{3h}) ($\Delta E = 3.25$ eV) than in $HaCl_5$ (C_{4v}) ($\Delta E = 3.12$ eV). The total overlap population for the D_{3h} case is 2.60 and for C_{4v} is 2.40 what indicates that D_{3h} hybridization is more favorable for covalent bonding. The dissociation energy calculations using the "counterpoise" scheme (with minimal ionized basis set) have shown close values of 14.51 and 15.60 eV, respectively for D_{3h} and C_{4v} cases. But taking into account still unsufficient accuracy of the DVH method for the total energy values one should not rely much on the values of the dissociation energies while the other characteristics of the electronic structure indicate that the D_{3h} symmetry probably is more advantageous for $HaCl_5$ than the C_{4v} one.

One way to prove experimentally the presence of one or the other structure could be feasible provided x-ray spectra of the short-lived molecules of hahnium were measured. The different geometrical (D_{3h} or C_{4v}) configurations of the five chlorines would give significantly different structure of their ns lines in x-ray spectra. The calculated 2s(Cl) lines for these two cases are shown in Fig. 9.

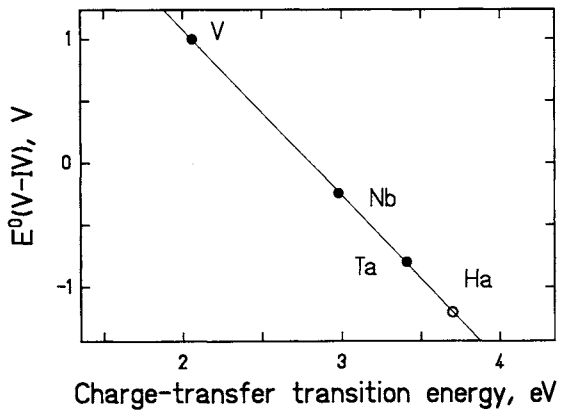

FIG. 8. Correlation between redox potentials E^0(V − IV) and energies of the lowest charge transfer transitions in MCl_5 (M = V, Nb, Ta, and Ha). {Data E^0(V − IV) for V, Nb, and Ta are from Ref. 34.} E^0(V − IV) for Ha equal to − 1.15 V is for $R_{ax}/R_{eq} = 2.42/2.28$ Å in $HaCl_5$.

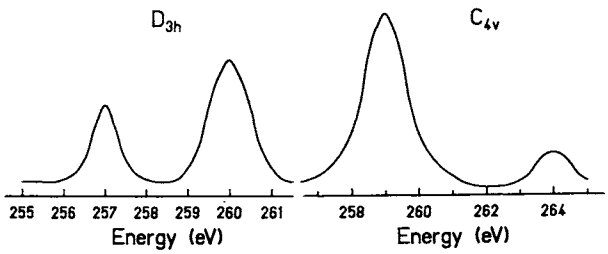

FIG. 9. Theoretical x-ray spectra for $HaCl_5$ [2s(Cl) lines].

VI. CONCLUSIONS

Results of the atomic MCDF calculations as well as most data of the present molecular calculations confirm the idea of hahnium being a typical member of the group 5 elements with its properties being determined by the valence $6d$ and $7s$ orbitals. In a number of physicochemical properties Ha continues the tendencies found for the lighter elements in the group. Thus there is a steady increase in atomic and ionic radii (with exception of Ta), gradual change in R_{max} of the valence orbitals, increase in ionization potentials $(0) - (5+)$, indicating the increasing stability of the pentavalent state down the group.

Molecular orbital calculations also confirm this fact. There is an increase in molecular ionization potentials, increase in energies of the first electronic charge-transfer transitions, and decrease in electron affinity provided relativistic bond contraction takes place.

Relativistic effects such as expansion (contraction) of the orbitals and their energetical stabilization (destabilization) introduce some peculiarities into charge-density distribution but the net result is the steady increase in covalency of the pentahalides and decrease in effective charges in going from Nb to Ta pentachlorides. The slight differences in the atomic electronic structure of element 105 compared to its analogs such as the availability of many closely spaced electronic configurations will hardly influence molecular properties due to the strong crystal field effect of the five chlorines. The value of the splitting of the d orbitals in the crystal field of the chlorines steadily increases in the group with $HaCl_5$ as a special case owing to strong relativistic contribution of $7s$ orbitals into bonding. This will result in the lower energies of the highest charge-transfer transitions in Ha compounds compared to Ta ones.

The electronic structure data confirm the specific position of Ta in the group. Ta obviously occupies such a position in the group where some effects are compensated by the others. Thus relativistic effects could be a reason for Ta having the same ionic radius (or bond length) as Nb, as it was in case of Zr, Hf, and Mo, W when relativistic contraction contributes to the dominating shell-structure effect of lanthanoid contraction.[28] In case of effective charges the relativistic stabilization of the valence s and $p_{1/2}$ orbitals is compensated by destabilization of d orbitals resulting in the values of effective charges being nearly equal for Nb and Ta. This specific electronic structure of Ta seems to be a reason of its chemical similarity to Nb while Ha should have some differences in its chemistry but in many aspects in line with the trends in the group.

The chemical bonding in tantalum pentachloride is probably stronger than in the other molecules under consideration because of both ionic and covalent contributions. The development of more precise relativistic methods may possibly allow exact values of the dissociation energies to be calculated.

ACKNOWLEDGMENTS

This work was supported by the Gesellschaft für Schwerionenforschung (GSI), Darmstadt. The authors would like to acknowledge several useful discussions of the experimental results on the chemistry of element 105 with Professor J. V. Kratz, Professor D. C. Hoffman, Dr. M. Schädel, Dr. H. W. Gäggeler, Dr. W. Brüchle, and Professor G. Ionova. They are also thankful to colleagues at the Physics Department of the University of Kassel for support at the initial stage of the calculations.

[1] B. Fricke and J. T. Waber, Actinides Rev. **1**, 433 (1971).
[2] B. Fricke, Struct. Bonding **21**, 89 (1975).
[3] J.-P. Desclaux and B. Fricke, J. Phys. **41**, 943 (1980).
[4] V. A. Glebov, L. Kasztura, V. S. Nefedov, and B. L. Zhuikov, Radiochim. Acta **46**, 117 (1989).
[5] (a) E. Johnson, B. Fricke, D. L. Keller, Jr., C. W. Nestor, Jr., and T. C. Tucker, GSI Scientific Report No. 89-1, 1988, p. 197; (b) E. Johnson, B. Fricke, O. L. Keller, Jr., C. W. Nestor, Jr., and T. C. Tucker, J. Chem. Phys. **93**, 8041 (1990); (c) B. Fricke and E. Johnson, Radiochim. Acta (to be published).
[6] D. T. Jost, H. W. Gäggeler, Ch. Vogel, M. Schädel, E. Jäger, B. Eichler, K. E. Gregorich, and D. C. Hoffman, Inorg. Chim. Acta **146**, 255 (1988).
[7] U. W. Scherer, J. V. Kratz, M. Schädel, W. Brüchle, K. E. Gregorich, R. A. Henderson, D. Lee, M. Nurmia, and D. C. Hoffman, Inorg. Chim. Acta **146**, 249 (1988).
[8] Yu. T. Chuburkov, V. Z. Belov, R. Tsaletka, M. R. Shalaevskii, and I. Zvara, Radiokhim. **11**, 394 (1969) [Sov. Radiochem. **11**, 386 (1969)].
[9] (a) I. Zvara, Y. T. Chuburkov, V. Z. Belov, G. V. Buklanov, B. B. Zakhvataev, T. S. Zvarova, O. D. Maslov, R. Caletka, and M. R. Shalaevsky, J. Inorg. Chem. **32**, 1885 (1970); (b) I. Zvara, V. Z. Belov, L. B. Chelnokov, V. P. Domanov, M. Hussonois, Yu. S. Korotkin, V. A. Schegolev, and M. R. Shalayevskii, Inorg. Nucl. Chem. Lett. **7**, 1109 (1971); (c) A. Türler and H. W. Gäggeler (private communication); (d) D. C. Hoffaman, Report No. LBL-29815, 1990.
[10] (a) I. Zvara, V. Aikhler, V. Z. Belov, T. S. Zvarova, Yu. S. Korotkin, M. R. Shalaevskii, V. A. Schchegolev, and M. Yussonnua, Radiokhim. **16**, 720 (1974) [Sov. Radiochem. **16**, 709 (1974)]; (b) I. Zvara, in *Transplutonium Elements*, edited by W. Müller and R. Lindner (North-Holland, Amsterdam, 1976), pp. 11–20; (c) I. Zvara, V. Z. Belov, V. P. Domanov, and M. R. Shalaevskii, Radiokhim. **18**, 371 (1976) [Sov. Radiochem. **18**, 328 (1976)]; (d) I. Zvara, in *Proceedings of the International School-Seminar on Heavy Ion Physics*, Dubna, 1987, p. 145 (unpublished); (e) H. W. Gäggeler, D. T. Jost, U. Baltensperger, Ya Nai-Qi, K. E. Gregorich, C. M. Gannett, H. L. Hall, R. A. Henderson, D. M. Lee, J. D. Li, M. J. Nurmia, D. C. Hoffman, A. Türler, Ch. Lienet, M. Schädel, W. Brüchle, J. V. Kratz, H. P. Zimmermann, and U. W. Scherer, Report PSI, PSI-Bericht Nr 49, 1989; (f) H. W. Gäggeler, D. T. Jost, J. Kovacs, U. W. Scherer, A. Weber, D. Vermeulen, J. V. Kratz, M. K. Gober, H. P. Zimmermann, M. Schädel, W. Brüchle, I. Zvara, A. Türler, K. E. Gregorich, R. A. Henderson, K. R. Czerwinski, B. Kadkhodayan, D. M. Lee, M. Nurmia, and D. C. Hoffman, Radiochim. Acta (in press).
[11] W. Brüchle, U. W. Scherer, J. V. Kratz, K. E. Gregorich, D. Lee, M. Nurmia, R. M. Chasterler, H. L. Hall, R. A. Henderson, and D. C. Hoffman, Inorg. Chim. Acta **146**, 267 (1988).
[12] (a) R. J. Silva, J. Harris, M. Nurmia, K. Eskola, and A. Ghiorso, Inorg. Nucl. Chem. Lett. **6**, 871 (1970); (b) E. K. Hulet, R. W. Lougheed, J. F. Wild, J. H. Landrum, J. M. Nitschke, and A. Ghiorso, J. Inorg. Nucl. Chem. **42**, 79 (1980).
[13] (a) K. E. Gregorich, R. A. Henderson, D. M. Lee, M. J. Nurmia, R. M. Chasteler, H. L. Hall, D. A. Bennett, C. M. Gannet, R. B. Chadwick, J. D. Leyba, D. C. Hoffman, and G. Herrmann, Radiochim. Acta **43**, 223 (1988); (b) J. V. Kratz, H. P. Zimmermann, U. W. Scherer, M. Schädel, W. Brüchle, K. E. Gregorich, C. M. Gannett, H. L. Hall, R. A. Henderson, D. M. Lee, J. D. Leyba, M. J. Nurmia, D. C. Hoffman, H. Gäggeler, D. Jost, U. Baltensperger, Ya Nai-Qi, A. Türler, and Ch. Lienert, *ibid.* **48**, 121 (1989).
[14] M. Schädel (Preprint No. GSI-89-72, October 1989).
[15] (a) C. E. Moore, *Atomic Energy Levels*, Natl. Stand. Ref. Data Ser. Natl. Bur. Stand., Washington, D.C., 1971; (b) C. E. Moore, *Ionization Potentials and Ionization Limits Derived from the Analyses of Optical Spectra*, Natl. Stand. Ref. Data Ser. Natl. Stand., Washington, D.C., 1970.
[16] L. Brewer, J. Opt. Soc. Am. **61**, 1101 (1971).

[17] R. D. Shannon, Acta Crystallogr. Sect. A **32**, 751 (1976).
[18] J. D. McDowell, US-AEC Report No. ORNL-4562, 1970.
[19] J. P. Desclaux, At. Data Nucl. Data Tables **12**, 311 (1973).
[20] A. Rosen and D. E. Ellis, J. Chem. Phys. **62**, 3039 (1975).
[21] A. Rosen, Int. J. Quantum Chem. **13**, 509 (1978); (b) J. Meyer, *ibid.* **33**, 445 (1988).
[22] J. Meyer, W.-D. Sepp, and B. Fricke, Comput. Phys. Commun. **54**, 55 (1989).
[23] R. S. Mulliken, J. Chem. Phys. **23**, 1833 (1955).
[24] A. A. Ischenko, T. G. Strand, A. V. Demidov, and V. P. Spiridonov, J. Mol. Struct. **43**, 227 (1978).
[25] A. Rosen and B. Fricke, Chem. Phys. Lett. **61**, 75 (1979).
[26] B. J. Krohn, W. B. Person, and J. Overend, J. Chem. Phys. **65**, 969 (1976).
[27] D. Brown, in *Comprehensive Inorganic Chemistry*, edited by J. C. Bailar (Pergamon, Oxford, 1973), Vol. 5, p. 187.
[28] P. Pyykkö and J. P. Desclaux, Chem. Phys. **34**, 261 (1978).
[29] See AIP document No. PAPS JCPSA-96-8367-8 for 8 pages of molecular orbitals for $NbCl_5$, $TaCl_5$, $HaCl_5$, and $PaCl_5$. Order by PAPS number and journal reference from American Institute of Physics, Physics Auxiliary Publication Service, 335 East 45th Street, New York, NY 10017. The price is $1.50 for each microfiche (60 pages) or $5.00 for photocopies of up to 30 pages, and $0.15 for each additional page over 30 pages. Airmail additional. Make checks payable to the American Institute of Physics.
[30] D. Brown, in *Comprehensive Inorganic Chemistry*, edited by J. C. Bailar (Pergamon, Oxford, 1973), Vol. 3, pp. 553–622.
[31] L. G. Hubert-Pfalzgraf, M. Postel, and J. G. Riess, in *Comprehensive Coordination Chemistry*, edited by G. Wilkinson (Pergamon, Oxford, 1978), Vol. 3, p. 589.
[32] *Gmelin Handbuch: Protactinium* (Springer, Berlin, 1977), Vol. 2, pp. 6 and 65.
[33] J. C. Slater, *The Self-Consistent Field for Molecules and Solids* (McGraw–Hill, New York, 1974), Vol. 4, Chap. 2.
[34] S. G. Bratsch, J. Phys. Chem. Ref. Data **18**, 1 (1989).